Access Channel Model for the Voltage Dependence of the Forward-running Na^+/K^+ Pump

ANJALI SAGAR and R. F. RAKOWSKI

From the Department of Physiology and Biophysics, University of Health Sciences/ The Chicago Medical School, North Chicago, Illinois 60064

ABSTRACT The voltage dependence of steady state current produced by the forward mode of operation of the endogenous electrogenic Na^+/K^+ pump in Na^+-loaded *Xenopus* oocytes has been examined using a two-microelectrode voltage clamp technique. Four experimental cases (in a total of 18 different experimental conditions) were explored: variation of external $[Na^+]$ ($[Na]_o$) at saturating (10 mM) external $[K^+]$ ($[K]_o$), and activation of pump current by various $[K]_o$ at 0, 15, and 120 mM $[Na]_o$ (tetramethylammonium replacement). Ionic current through K^+ channels was blocked by Ba^{2+} (5 mM) and tetraethylammonium (20 mM), thereby allowing pump-mediated current to be measured by addition or removal of external K^+. Control measurements and corrections were made for pump current run-down and holding current drift. Additional controls were done to estimate the magnitude of the inwardly directed pump-mediated current that was present in K^+-free solution and the residual K^+-channel current. A pseudo two-state access channel model is described in the Appendix in which only the pseudo first-order rate coefficients for binding of external Na^+ and K^+ are assumed to be voltage dependent and all transitions between states in the Na^+/K^+ pump cycle are assumed to be voltage independent. Any three-state or higher order model with only two oppositely directed voltage-dependent rate coefficients can be reduced to an equivalent pseudo two-state model. The steady state current–voltage (*I-V*) equations derived from the model for each case were simultaneously fit to the *I-V* data for all four experimental cases and yielded least-squares estimates of the model parameters. The apparent fractional depth of the external access channel for Na^+ is 0.486 ± 0.010; for K^+ it is 0.256 ± 0.009. The Hill coefficient for Na^+ is 2.18 ± 0.06, and the Hill coefficient for K^+ (which is dependent on $[Na]_o$) ranges from 0.581 ± 0.019 to 1.35 ± 0.034 for 0 and 120 mM $[Na]_o$, respectively. The model provides a reasonable fit to the data and supports the hypothesis that under conditions of saturating internal $[Na^+]$, the principal voltage dependence of the Na^+/K^+ pump cycle is a consequence of the existence of an external high-field access channel in the pump molecule through which Na^+ and K^+ ions must pass in order to reach their binding sites.

Address correspondence to Dr. R. F. Rakowski, Department of Physiology and Biophysics, University of Health Sciences/The Chicago Medical School, 3333 Green Bay Road, North Chicago, IL 60064.

J. GEN. PHYSIOL. © The Rockefeller University Press · 0022-1295/94/05/0869/26 $2.00
Volume 103 May 1994 869–894

INTRODUCTION

Over the past few years the voltage dependence of the steady-state current produced by the operation of the electrogenic Na^+/K^+ pump has been measured under a variety of experimental conditions in various preparations: e.g., squid giant axons (Rakowski, Gadsby, and De Weer, 1989); cardiac myocytes (Nakao and Gadsby, 1989); and amphibian oocytes (Lafaire and Schwarz, 1986; Eisner, Valdeolmillos, and Wray, 1987; Rakowski and Paxson, 1988; Wu and Civan, 1991). However, only in a few cases has an attempt been made to fit the steady state current–voltage (*I-V*) data to a model and extract quantitative information from the fit parameters (Nakao and Gadsby, 1989; Vasilets, Ohta, Naguchi, Kawamura, and Schwarz, 1993). Hansen, Gradmann, Sanders, and Slayman (1981) have described a pseudo two-state model for an electrogenic pump cycle that results from the simplification of all possible multistate cycles in which only a single step is voltage dependent. Nakao and Gadsby (1989) have described the $[Na]_o$ and $[K]_o$ dependence of steady state Na^+/K^+ pump current using this model. In their analysis it was assumed that the voltage dependence of pump current is governed by a single asymmetrical Eyring barrier with voltage-dependent forward and backward rate coefficients for Na^+ translocation. However, recent evidence suggests that only the backward rate coefficient is voltage dependent. Based on florescence studies with membranes labeled with electrochromic dyes, it has been postulated that the binding sites for Na^+ and K^+ are buried in the membrane dielectric and are connected to the external medium by a narrow access channel (Stürmer, Bühler, Apell, and Läuger 1991*a*, *b*). Further evidence has been provided based on the voltage dependence of electroneutral Na^+/Na^+ exchange that Na^+ ions reach their binding sites deep in the pump molecule through a high field access channel (Gadsby, Rakowski, and De Weer, 1993). For an access channel the pseudo first-order external Na^+ binding rate coefficient is voltage dependent as a result of the voltage drop within the access channel influencing the effective concentration of Na^+ at its external binding site. Because the rate of ion movement within the access channel is expected to occur orders of magnitude faster than the rate of ion release, the rate coefficient for release of external Na^+ is assumed to be voltage independent. This asymmetrical voltage dependence of the external Na^+ binding and release rate coefficients has been shown directly by measurement of the relaxation rate of pre–steady state transient currents under Na^+/Na^+ exchange conditions (Rakowski, 1993; cf. Nakao and Gadsby, 1986). It has also been established that there is a second voltage-dependent step in the K^+ translocating pathway that explains the negative slope in the forward Na^+/K^+ pump *I-V* relationship when $[K]_o$ is reduced below saturation (Rakowski, Vasilets, LaTona, and Schwarz, 1991; Gadsby, Nakao, Bahinski, Nagel, and Suenson, 1992). Because the apparent affinity for activation of forward pump current by $[K]_o$ is voltage dependent (Rakowski et al., 1991), it is reasonable to postulate that the external binding sites for K^+ are also located within an access channel. The goal of this study is to reexamine the $[Na]_o$ and $[K]_o$ dependence of steady-state Na^+/K^+ pump current using an access channel model. In that no adequately large and completely consistent data set is available in the literature, we have redetermined the steady state pump *I-V* relationships for *Xenopus* oocytes for four comparable experimental cases. Because this data set is

self-consistent, it allows a simultaneous least-squares fit to be made to obtain values for model parameters that are common to all the experimental cases. A three-state model for the pump is proposed, assuming the existence of an external access channel for Na^+ and K^+. Because only two oppositely directed rate coefficients of this three-state access channel model are voltage dependent, the model can be reduced to a pseudo two-state model that can be fit to *I-V* relationships obtained under various experimental conditions (see Appendix). The fitting procedure yields estimates for the fractional depth of the external access channel and Hill coefficients for Na^+ and K^+, and various combinations of the voltage independent rate coefficients of the pseudo two-state model.

Two abstracts of the results reported here have been published (Sagar, Wallner, and Rakowski, 1993; Sagar and Rakowski, 1993).

METHODS

Preparation of Oocytes

Adult female African clawed frogs (*Xenopus laevis*) obtained from Xenopus I (Ann Arbor, MI) were maintained on a high-protein diet in fresh water tanks. Frogs were anesthetized by immersion in crushed ice for 30 min until unresponsive to tactile stimulation. Pieces of the ovary were removed through an abdominal incision. To remove follicular cells, oocytes were treated for ~2 h with collagenase (0.6–0.8 U/ml) in oocyte Ringer solution (87.5 mM NaCl, 2.5 mM KCl, 1.0 mM $MgCl_2$, 5.0 mM Tris/HEPES buffer, pH 7.6). Intracellular [Na^+] was elevated either by incubation for 1 h at room temperature in a Na^+-loading solution (90 mM Na-sulfamate, 5.0 Tris/HEPES buffer, 2.5 mM Na-citrate) (LaTona, 1990; Rakowski, et al., 1991) or by overnight incubation at 15–16°C in K^+-free oocyte Ringer's solution (87.34 mM NaCl, 0.74 mM $CaCl_2$, 0.66 mM $NaNO_3$, 0.82 mM $MgSO_4$, 2.4 mM $NaHCO_3$, 5 mM Tris/HEPES, pH 7.6).

Solutions

All solutions were designed to minimize non–pump-mediated currents. Tetraethylammonium (TEA) (20 mM) and Ba^{2+} (5 mM) were present to block K^+ channel currents. Ni^{2+} (2 mM) was present to block Na^+/Ca^{2+} exchange and has been shown to have no effect on forward Na^+/K^+ pump current in oocytes (Rakowski et al., 1991). All solutions also contain 5 mM Tris/HEPES and had a pH of 7.6. The experimental solutions contain different amounts of NaCl, tetramethylammonium Cl (TMACl), and KCl totaling 130 mM. For example, the solution referred to as 10 K 120 Na contained 10 mM K^+, 120 mM Na^+, and no TMACl and the 0 K 0 Na solution contained 130 mM TMACl substituting for both NaCl and KCl.

Electrophysiological Measurements

A two microelectrode voltage clamp system (model OC725; Warner Instruments, Hamden, CT) was used to maintain the holding potential at −40 mV. *I-V* relationships were measured over the range −160 to 0 mV with a down-up-down voltage staircase in which each step was 5 mV in amplitude and 0.5 s in duration. The current-passing electrodes (shielded by Al foil) were filled with 2 M K citrate and had resistances of 1–4 MΩ. Intracellular voltage recording electrodes were filled with 3 M KCl and also had resistances of 1–4 MΩ. Data were collected using a commercially available analog-to-digital (A-D) converter system (TL-1 DMA interface, 100 kHz; Axon Instruments, Inc., Burlingame, CA) and software written in QuickBASIC (Microsoft Corp., Redmond, WA) for an IBM-compatible computer system. Analysis and graphical

presentation of the data were done with SIGMAPLOT software (version 5.0; Jandel Scientific, Corte Madera, CA).

RESULTS

Experimental Protocols for the Measurement of Steady State Pump Current

Figs. 1 and 2 show complete experiments for the measurement of steady-state pump current either at a constant $[Na]_o$ (Fig. 1) or at various $[Na]_o$ at constant test $[K]_o$ (Fig. 2). Each spikelike event is the current recorded during a down-up-down voltage staircase from −160 to 0 mV. It is typical that the oocytes tighten as each experiment continues as shown by the decrease in the amplitude of the spikes during the experiment. In order to estimate run-down of the pump current magnitude with time, the first solution change of the experiment and the last solution change that activated pump current were always to the same $[K]_o$ and $[Na]_o$, (2.5 mM $[K]_o$ Na^+-free, *c*, *d*, *w*, and *x* in Fig. 1; 10 mM $[K]_o$, 120 mM $[Na]_o$, *e*, *f*, *cc*, and *dd* in Fig. 2). We corrected for run-down by multiplying each *I-V* relationship by an appropriate scaling factor calculated from the pump current magnitude measured from the first and last solution change. If it was necessary to terminate the protocol before the last change in $[K]_o$, a correction for the average run-down rate from all similar experiments was applied to the data from each intermediate $[K]_o$ change. Other experiments established that the pump current runs down approximately linearly with time (data not shown). Although the current record is quite stable in each condition, the holding current may drift somewhat with time. To correct for this drift, two *I-V* readings were done in each solution (5 min apart). A linear correction for drift could then be calculated from the difference between each pair of *I-V* readings (Rakowski et al., 1989).

Fig. 1 shows the protocol for determining *I-V* relationships at a fixed $[Na]_o$ ($[Na]_o = 0$ in this case) at various $[K]_o$. Pump current was measured by subtraction of *I-V* data in K^+-free solution from data at various $[K]_o$. The order of intervening $[K]_o$ changes was varied randomly between experiments (in the experiment shown in Fig. 1, $[K]_o$ changes were made in increasing order). Each test $[K]_o$ was always bracketed by measurements in K^+-free solution to allow both forward and backward subtractions in time to be made. Fig. 2 shows the protocol for determining *I-V* relationships at various $[Na]_o$. Because measurements of the *I-V* difference at a given $[Na]_o$ require two solution changes (one to change to the desired $[Na]_o$, and the other to change from 0 to 10 mM K^+ to activate the pump), it was not possible to examine more than four values of $[Na]_o$ in the same oocyte routinely because of the long duration of the experiment. Therefore, this set of data was collected in two separate protocols. That is, one set of experiments measured *I-V* relationships at 120, 60, 30, and 0 mM $[Na]_o$. A separate set of experiments was done to measure *I-V* relationships at 120, 15, and 7.5 mM $[Na]_o$.

Control Experiments

At the end of successful experiments two controls were usually done. Since removal of extracellular K^+ prevents the Na^+/K^+ pump from operating in the forward direction, but does not prevent reverse operation of the pump, we tested whether any reverse

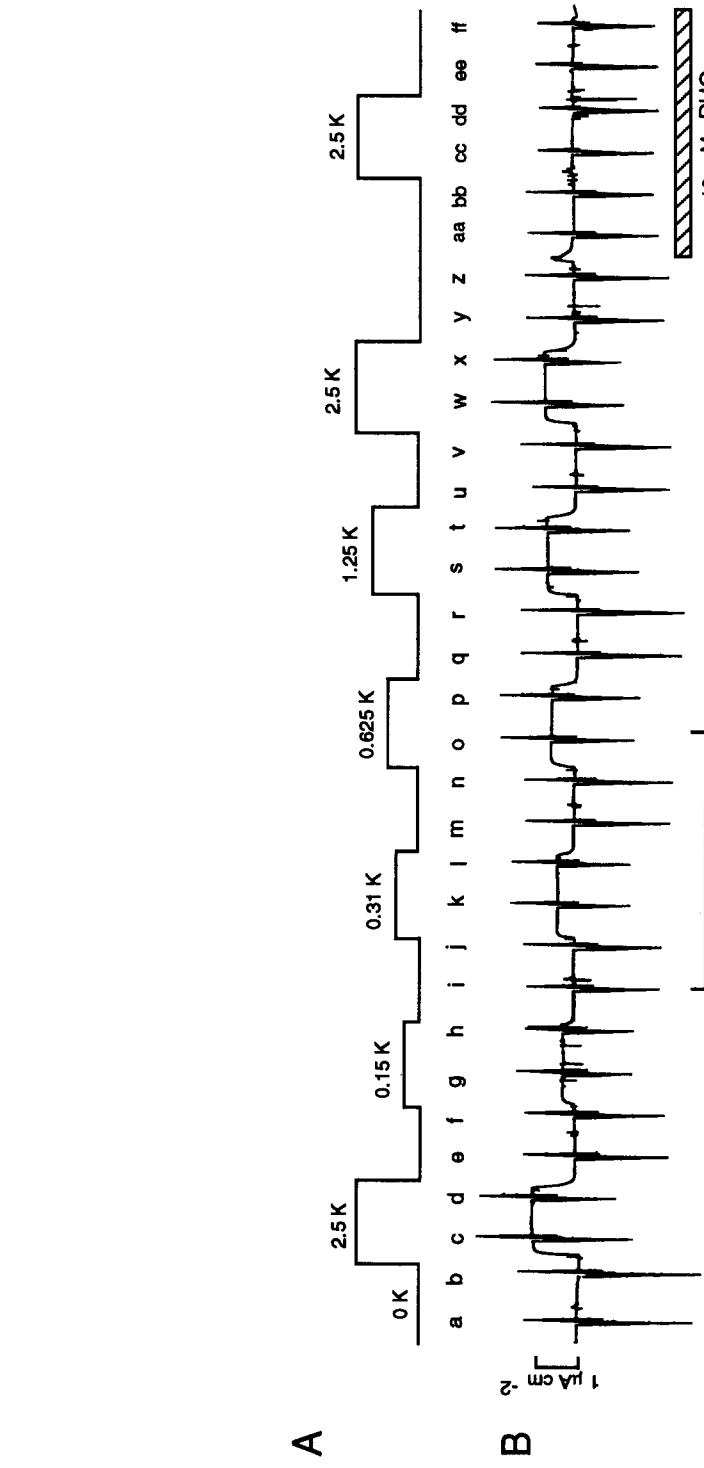

FIGURE 1. Protocol for a typical experiment at fixed $[Na]_o$. (*A*) $[K]_o$ changes during an experiment in Na^+-free solutions (TMA substitution). $[K]_o$ was varied between 2.5 and 0.15 mM (TMACl substitution for KCl). Pump current was measured by subtraction of *I-V* data in K^+-free solution from data at various $[K]_o$. Each new $[K]_o$ was bracketed by measurements in K^+-free solution. For example, *I-V*'s at 0.625 mM $[K]_o$ (*o* and *p*) are bracketed by *I-V*'s in 0 mM K^+-free solution (*m*, *n*, *q*, and *r*). (*B*) Chart recording of current during the experiment. Each spikelike event shows the current recorded during a down-up-down voltage staircase from −160 to 0 mV. Note that there is a small artifact in the current record right before the addition of DHO (between *z* and *aa*). This was most likely due to an inadvertent static electricity discharge that occurred when changing between these solutions and did not occur in other experiments. Control measurements were made in the presence of 10 μM DHO, which was added at the end of the experiment for the duration shown by the hatched bar. The duration of this experiment was ~3 h; each *I-V* determination was 5 min apart.

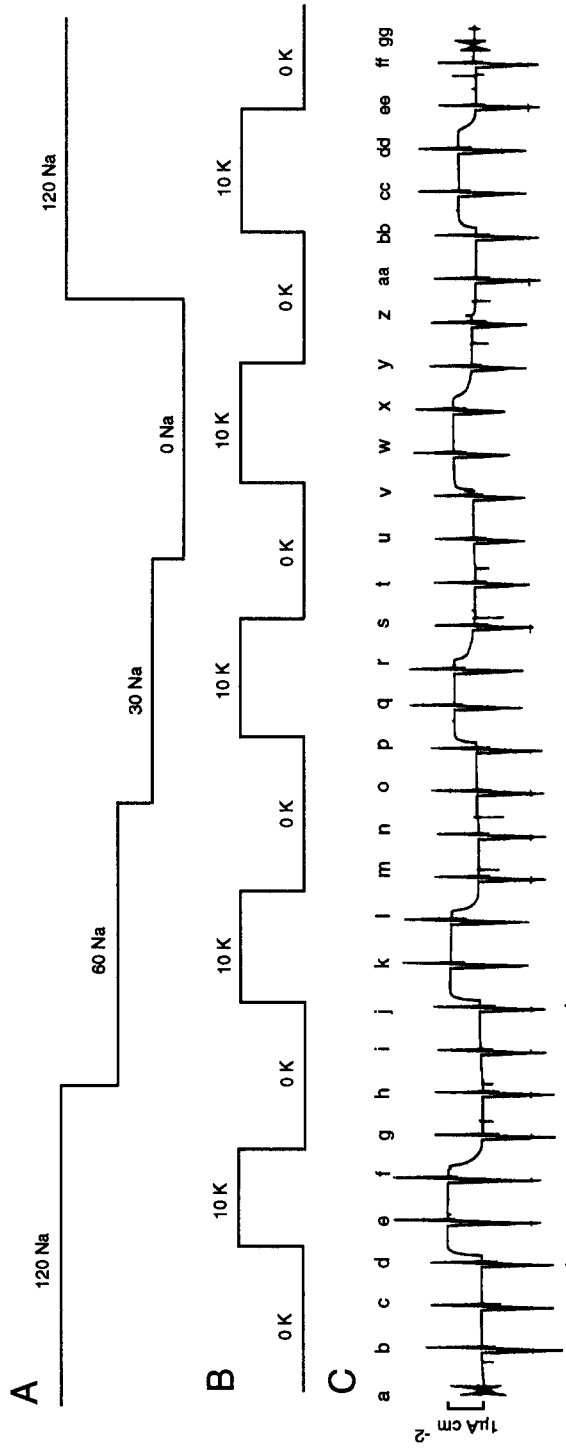

FIGURE 2. Protocol for an experiment in 10 mM K^+ and various $[Na]_o$. (*A*) $[Na]_o$ changes to concentrations between 120 and 0 mM during the experiment (TMA substitution). (*B*) Sequence of external K^+ addition and removal to turn the pump on and off. K^+-sensitive pump current was measured by subtraction of *I-V* data in K^+-free solution from data in 10 mM K^+. For each $[Na]_o$, *I-V* measurements are first made in K^+-free solution, then 10 mM $[K]_o$ to activate the pump, and then bracketed by a measurement in K^+-free solution again. For example, in the case of 30 mM Na^+, two *I-V* relationships are obtained in K^+-free solution before (*o* and *p*) and after (*s* and *t*) the application of 10 mM $[K]_o$ (*q* and *r*). (*C*) Chart recording of current during the experiment. The duration of this experiment was also ~3 h. The small current deflections at the very beginning (*a*) and the end of the experiment (*gg*) represent responses to a series of 0.5-s voltage pulses incremented by 0.5 mV in each successive pulse up to ±5 mV from the holding potential. The slope conductance calculated for (*a*) was 22.2 μS cm^{-2} and for (*gg*) was 14.5 μS cm^{-2} consistent with a gradual tightening of passive conductance during the experiment.

pump current was present in K^+-free solution. Dihydroouabain (DHO, 10 μM) was added to K^+-free solution after completion of the K^+-activation protocol (from *z* to *aa* in Fig. 1). Little or no current change was observed at the holding potential (−40 mV). A second type of control measurement was done to determine whether any significant K^+ channel-mediated current was present that would contaminate the pump current measurements. External solution changes from a high $[K]_o$ (2.5 or 10 mM) to K^+-free solution were made in the presence of 10 μM DHO (from *bb* to *cc* in Fig. 1) to determine if any significant non–pump-mediated K^+-sensitive current was present. A final set of control measurements was made by changing to K^+-free solution in the presence of DHO (from *dd* to *ee* in Fig. 1). The magnitude of the residual K^+ channel–mediated current that was not blocked by Ba^{2+} and TEA was usually negligibly small.

Steady-State Na^+/K^+ Pump I-V *Relationships in Na^+-free Solution*

Pump current measured in Na^+-free solutions at various $[K]_o$, ranging from 0.15 to 2.5 mM is shown in Fig. 3 *A*. Under these conditions, there is a negative slope in the *I-V* relationship of the pump that results from the existence of a second voltage-dependent step in the Na^+/K^+ pump cycle (presumably in the K^+ half of the cycle because the experiments were done in Na^+-free solution). A negative slope in Na^+-free conditions was first seen by LaTona (1990), and was investigated by Rakowski et al. (1991). The pump current decreases with depolarization as expected from a reduction of the rate coefficient for binding of external K^+. That is, depolarization is expected to reduce the effective concentration of K^+ at its external binding site. Eq. A19 is the pseudo two-state current equation for this Na^+-free case. Eq. A19 was fitted to the *I-V* data in Fig. 3 *A* and is shown by the dashed lines. The fitting procedure gave the following parameter values (±SE): $FN\rho a = 0.995 \pm 0.029$ μA cm^{-2}, $\bar{c}/a = 0.77 \pm 0.04$ $mM^{-\gamma_K}$, $\gamma_K = 0.822 \pm 0.027$, and $\lambda_K = 0.280 \pm 0.007$. The solid lines in Fig. 3 *A* were calculated from the best-fit parameters obtained from a simultaneous fit to all of the *I-V* data in this paper (see Discussion). Control measurements in this group of oocytes were done when possible. Addition of 10 μM of DHO in Na^+- and K^+-free solution (Fig. 3 *B*) produced inhibition of a small (mostly) inwardly directed current. This current was previously described by Rakowski et al., 1991. The extent to which this current represents a possible source of experimental error will be considered in the Discussion. Fig. 3 *C* demonstrates that there was virtually no K^+-sensitive current that is not pump mediated. For these control data, K^+-sensitive current that is not mediated by the Na^+/K^+ pump is at most a tenth of the maximum pump current. TEA (20 mM) and Ba^{2+} (5 mM) were present in all solutions to minimize such passive K^+-sensitive currents. The data in Fig. 3 *A* are replotted in Fig. 3 *D* as a function of $[K]_o$ for 25-mV increments of membrane potential. The solid lines represent the K^+-activation form of the Hill equation (Eq. A24) calculated from the overall best-fit parameters. The value of I_{max} used to calculate the normalized pump current was taken to be the value of $FN\rho a$ calculated from the overall fit in Fig. 3 *A*. The inset shows the monoexponential increase in K_K with voltage calculated from Eq. A23 and the parameter values obtained from the overall least squares fitting procedure.

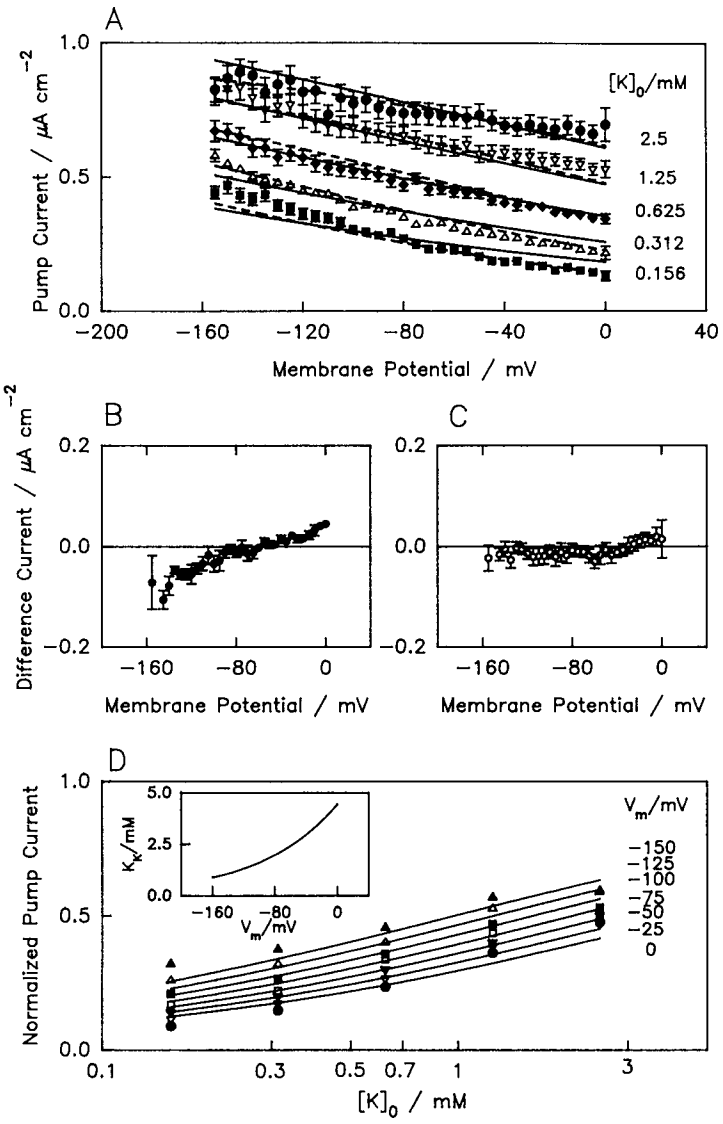

FIGURE 3. A. Pump current measured in Na^+-free solution at various $[K]_o$. $[K]_o$ was varied between 2.5 and 0.15 mM (TMACl substitution for KCl): (●) 2.5 mM K^+, (▽) 1.25 mM K^+, (◆) 0.625 mM K^+, (△) 0.312 mM K^+, and (■) 0.156 mM K^+. Data from 10 oocytes. (*B*) Mean values of control measurements of DHO-sensitive current in K^+-free solution (e.g., *z* − *aa* in Fig. 1). (*C*) Mean values of control measurements of K^+-sensitive current that is not pump mediated (e.g., *cc* − *bb* and *dd* − *ee* in Fig. 1). Control experiments (*B* and *C*) were successfully completed in 3 out of the 10 oocytes from *A*. SEM bars not shown when smaller than the symbols. (*D*) Normalized data from *A* replotted at 25-mV increments as a function of $[K]_o$. *Inset:* K_K calculated from Eq. A23. See text for values of the fit parameters.

Normalized Na^+/K^+ Pump I-V *Relationships at Various $[Na]_o$ and High $[K]_o$*

Fig. 4 shows *I-V* measurements made at saturating $[K]_o$ (10 mM) and various $[Na]_o$ ranging from 7.5 to 120 mM. The data were normalized to the value of pump current measured at 0 mV. Pump current is approximately a sigmoid function of voltage under these conditions, saturating at positive voltages and decreasing with hyperpolarization. As $[Na]_o$ is decreased, the midpoint voltage of the *I-V* relationship is shifted to more negative voltages. This is similar to the results of Nakao and Gadsby (1989). The solid lines in Fig. 4, *A* and *B*, were obtained from a normalized form of Eq. A26 (see figure legend) and the parameter values obtained from the overall fitting procedure. Fig. 4 *C* shows the data in Fig. 4, *A* and *B*, replotted as a function of $[Na]_o$ for 25-mV increments of voltage. The solid lines in Fig. 4 *C* connect points that are calculated from the Na^+ inhibition form of the Hill equation (Eq. A28) normalized to the current expected at 0 mV $[I(0)]$: $I/I(0) = K_N^{\gamma N}/(K_N^{\gamma N} + [Na]_o^{\gamma N})$, where $K_N^{\gamma N}$ is given by Eq. A27. The values of γ_K given in Table II (q.v.) were used for each $[Na]_o$. The inset in Fig. 4 *C* shows that K_N decreases with membrane hyperpolarization from a value of ~300 mM at 0 mV as calculated from Eq. A27 and the overall best-fit parameters for these data.

Steady-State Pump I-V *Relationships at 120 mM $[Na]_o$*

At 120 mM $[Na]_o$ and various $[K]_o$, the steady-state pump *I-V* relationship increases with depolarization over the voltage range −120 to 0 mV (Fig. 5 *A*). Rakowski et al. (1991) have shown, however, that there is a region of negative slope if a more positive voltage range is examined. The *I-V* relationships in Fig. 5 *A* show the increase of current amplitude with increasing $[K]_o$ expected for activation of forward pump current by $[K]_o$. The solid lines are calculated from Eq. A14 and the overall best-fit parameters. Fig. 5 *B* shows the control measurements for K^+-sensitive current that was not pump mediated. In these cases, as in Fig. 3, this nonpump current was also about one-tenth of the maximum forward-running pump current at membrane potentials close to 0 mV.

Fig. 5 *D* shows the data from *A* replotted as a function of $[K]_o$ at 20 mV increments. The solid lines are calculated from Eq. A24 and the parameters obtained from the overall least squares fit. Fig. 5 *C* shows the voltage dependence of K_K calculated from Eq. A25 using the overall fit parameters. Although Eq. A28 predicts a U-shaped relationship, this behavior is not apparent in the voltage range examined. Experiments designed to examine this predicted behavior are discussed below.

Steady-State Pump I-V *Relationships at 15 mM $[Na]_o$*

Fig. 6 *A* shows steady-state pump *I-V* relationships at low $[Na]_o$ (15 mM) and various $[K]_o$, ranging from 0.625 to 2.5 mM. In this case both a region of positive and negative slope in the *I-V* relationship are apparent, which requires that at least two steps in the pump cycle be voltage dependent. This complex behavior can be demonstrated in low $[Na]_o$ and below saturation of $[K]_o$. It has also been seen by Gadsby et al. (1992) in cardiac myocytes. The solid lines represent the fit calculated from Eq. A14 using the overall best-fit parameters. Fig. 6, *B* and *C*, shows the DHO-sensitive and nonpump K^+-sensitive control measurements from oocytes of this

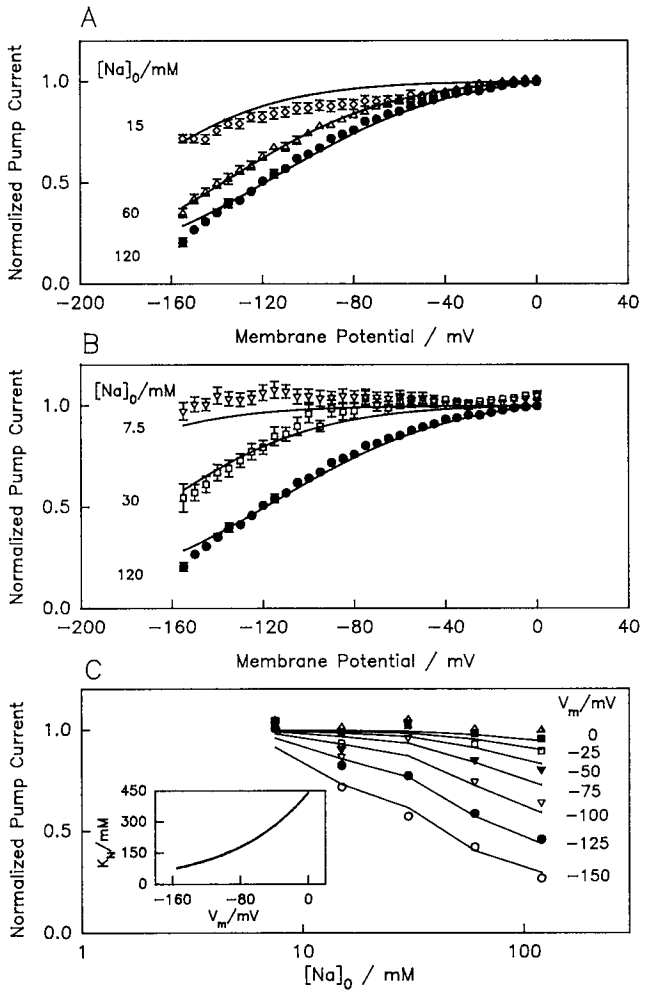

FIGURE 4. Normalized *I-V* relationships in 10 mM $[K]_o$ at various $[Na]_o$. $[Na]_o$ was varied between 120 and 7.5 mM. Pump current was measured by subtraction of the current in K^+-free solution from that in 10 mM K^+ solution. After the current difference was corrected for drift, it was normalized by dividing by the K^+-sensitive current measured at 0 mV. (*A*) $[Na]_o$ in 10 oocytes was varied between 120 (●), 60 (△), and 15 (◇) mM. (*B*) $[Na]_o$ in eight oocytes was varied between 120 (●), 30 (□), and 7.5 (▽) mM. SEM bars not shown when smaller than the symbols. The data in *A* and *B* were fit to Eq. A29 normalized to the value of current at 0 mV [*I*(0)], where $I(0) = FN\rho a/\{1 + (\bar{b}[Na]_o^{\gamma N}/\bar{c}[K]_o^{\gamma K})\}$. (*C*) Normalized current as a function of $[Na]_o$ at various membrane potentials. (*Inset*) Calculated values of K_N (Eq. A28) as a function of membrane potential using the least squares parameters obtained from the overall curve fit. See text for details of the curve fitting procedure and Tables I–III for values of the overall fit parameters.

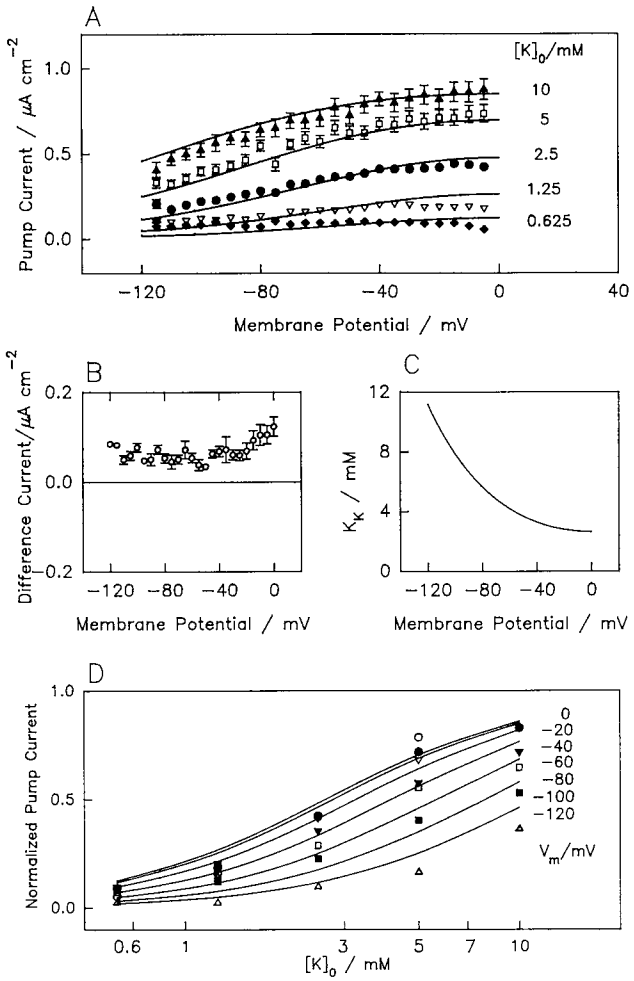

FIGURE 5. (*A*) Pump current measured in 120 mM $[Na]_o$ at various $[K]_o$. $[K]_o$ was varied between 10 and 0.625 mM. Pump current was measured in eight oocytes by subtraction of the current in K^+-free solution from that in various $[K]_o$: 10 (▲), 5 (□), 2.5 (●) 1.25 (△), and 0.625 (◆) mM. (*B*) Control estimate of K^+-sensitive current that is not pump mediated. Data from three of the eight oocytes in *A*. SEM bars not shown when smaller than the symbols. (*C*) K_K (Eq. A23) calculated from the overall fit parameters. (*D*) Normalized data from *A* replotted at 20-mV increments as a function of $[K]_o$. See text for further details.

group in which it was possible to make these control measurements. Fig. 6 *D* shows the data in Fig. 6 *A* replotted as a function of $[K]_o$ for 25-mV increments of membrane potential. The normalized current was obtained by dividing by the theoretical maximum current ($FN\rho a$) that was calculated from the overall fit in Fig. 6 *A*. The solid lines are calculated from the Hill equation (Eq. A24) where the half saturation concentration (K_K) is given by Eq. A25 and the parameter values are obtained from the overall fit. The inset shows that at 15 mM $[Na]_o$ K_K has a minimum near −90 mV. The U-shaped voltage dependence of K_K predicted by Eq. A25 is clear in this case of low $[Na]_o$ and $[K]_o$.

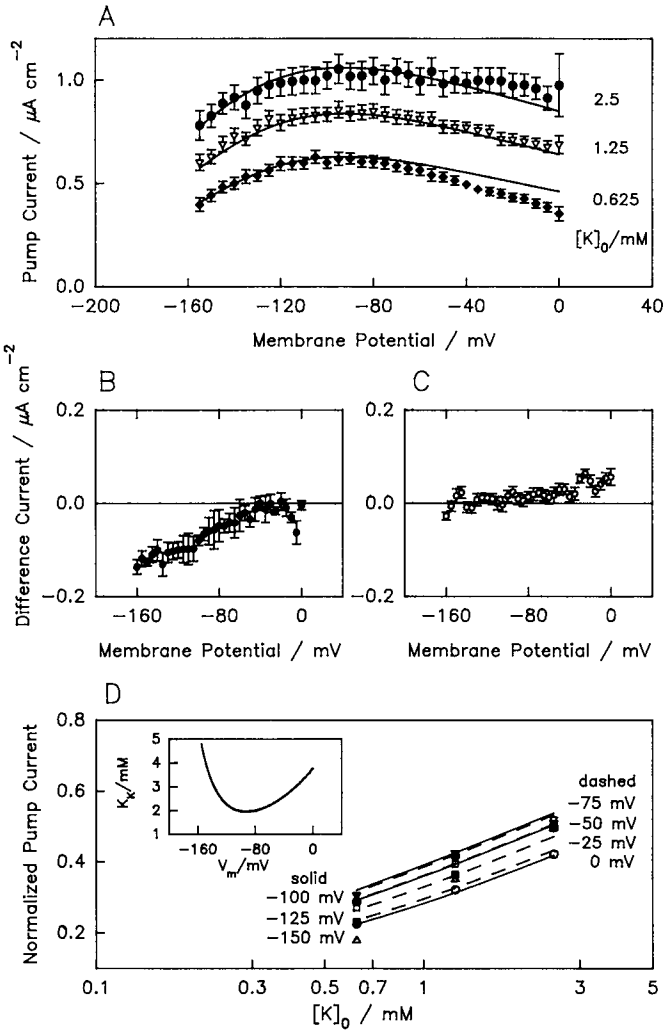

FIGURE 6. (*A*) Pump current measured in 15 mM $[Na]_o$ at various $[K]_o$. $[K]_o$ was varied between 2.5 and 0.625 mM in 12 oocytes: 2.5 (●), 1.25 (▽), and 0.625 (◆) mM. (*B*) Control measurements of DHO-sensitive current. (*C*) Control measurement of K^+-sensitive current that is not pump mediated. Control experiments (*B* and *C*) were done in 3 out of 12 oocytes from *A*. SEM bars not shown when smaller than the symbols. (*D*) Normalized current as a function of $[K]_o$ at various membrane voltages. (*Inset*) K_K (Eq. A23) calculated from the overall fit parameters.

DISCUSSION

Three-State Access Channel Model

A schematic representation of a three-state access channel model for the operation of the Na^+/K^+ pump is shown in Fig. 7 *A*. The model is intended to represent only the interactions of Na^+ and K^+ with their external-facing binding sites in the pump

molecule. It does not consider the possible existence of an access channel for binding of internal Na^+ since in these experiments the oocytes were Na^+ loaded and, therefore, the internal [Na^+] should be near saturation. Furthermore, it is assumed that all of the transitions between pump states are voltage independent. Voltage dependence of the pump cycle comes about as a consequence of the voltage-dependent increase in the probability of finding an external Na^+ or K^+ ion at its binding locus (λ) by rapid equilibration of Na^+ and K^+ within an external high-field access channel (Läuger, 1991, p 83). The effective concentrations of Na^+ and K^+ at their binding sites are increased by membrane hyperpolarization according to a Boltzmann distribution (Eqs. A1 and A2) in which λ_N and λ_K represent the fraction of the membrane potential (V) traversed by the ions to reach their binding sites (apparent well-depth). The pseudo first-order rate coefficients for binding of Na^+ and K^+ (k_{21} and k_{23}, respectively) are voltage dependent as a consequence of the voltage dependence of the effective concentrations of Na^+ and K^+ at their binding sites (Eqs. A3 and A4).

The kinetic model shown in Fig. 7 *A* is similar to that used by Andersen, Silveira, and Steinmetz (1985) to describe the pH and voltage dependence of proton transport in a tight urinary epithelium. It is not necessary, however, to postulate the existence of an aqueous antechamber in which a local concentration of the transported ion is established. We may instead regard the probability of finding the transported ion at its binding locus as an effective concentration and write Eqs. A1 and A2 analogous to Eq. A16 of Andersen et al. (1985). Vasilets et al. (1993) have also employed a kinetic model similar to that described here to describe their steady state *I-V* data. The assumption that the movements of Na^+ and K^+ within the access channel are rapid compared to the subsequent transitions of the enzyme and that the ions are at an equilibrium distribution within the channel leads to an important characteristic of access channel models, namely the kinetic equivalence of changes in substrate concentration and of membrane voltage. That is, changing the external concentration of the transported substrate should simply shift the position of the *I-V* relationship along the voltage axis without changing the maximum value of current or shape of the curve. For a change in external [K] from $[K]_1$ to $[K]_2$, Eq. A22 predicts a change in the midpoint voltage $\Delta\overline{V}_K$ given by

$$\Delta\overline{V}_K = \frac{RT}{\lambda_K F} \ln\left\{\frac{[K]_2}{[K]_1}\right\} \tag{1}$$

The value of λ_K, then, is not only determined from the steepness of an individual *I-V* relationship, but also from the shift that occurs when $[K]_o$ is changed. An analogous expression can be derived for the shift in midpoint voltage of the *I-V* relationship when $[Na]_o$ is changed at high external $[K]_o$:

$$\Delta\overline{V}_N = \frac{RT\gamma_N}{(\lambda_K\lambda_K - \lambda_N\lambda_N)F} \ln\left\{\frac{[Na]_2}{[Na]_1}\right\} \tag{2}$$

A similar relationship was derived by Gadsby et al. (1993) to describe the change in midpoint voltage of ^{22}Na efflux when $[Na]_o$ is changed under conditions of Na^+/Na^+ exchange. For such K-free conditions the $\gamma_K\lambda_K$ term is zero.

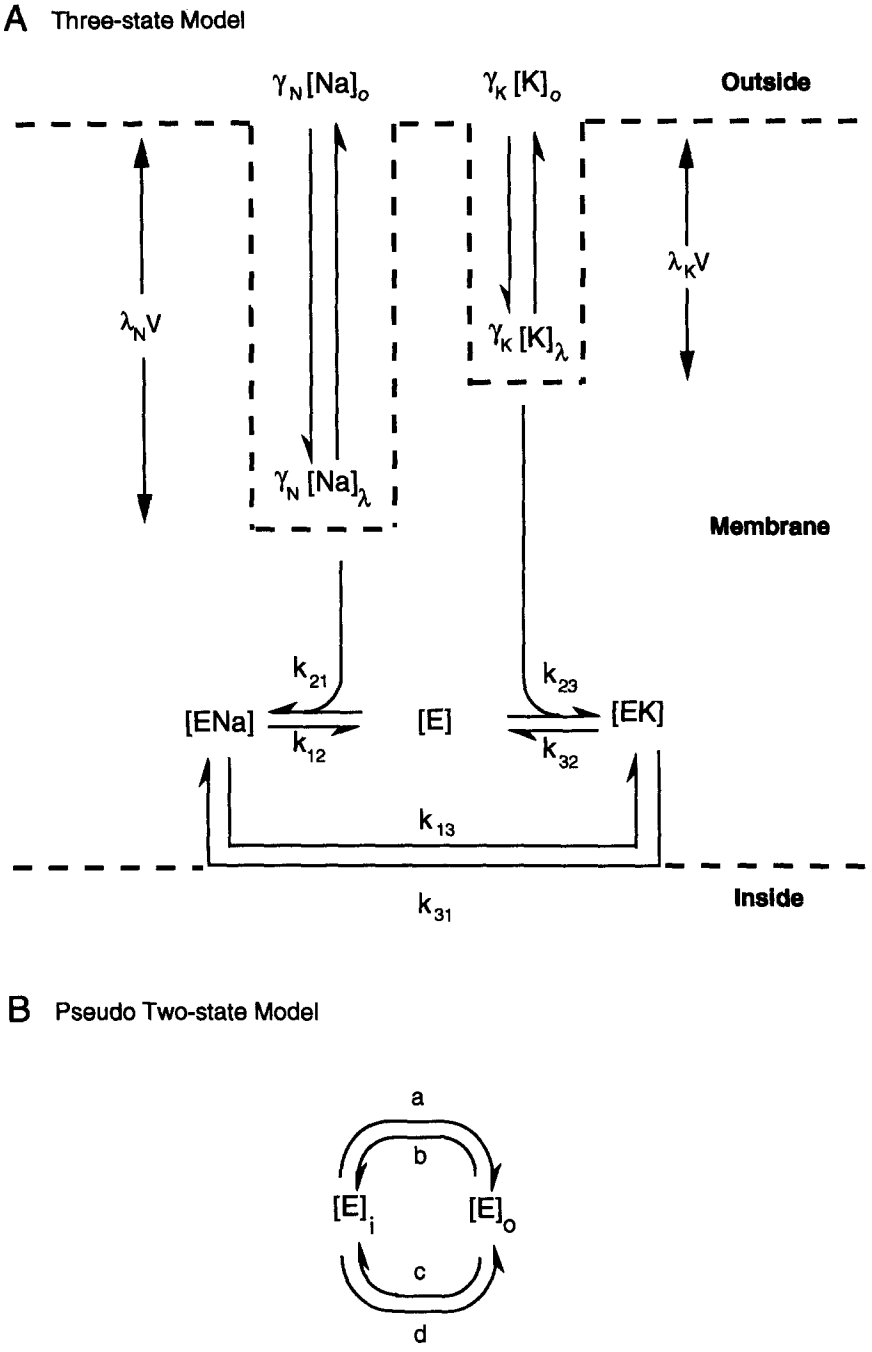

FIGURE 7. Kinetic models of pump operation. (*A*) Three-state model of steady-state operation of the Na^+/K^+ pump. [*E*Na] represents a state with Na^+ bound to the enzyme; [*E*K] represents a state with K^+ bound to the enzyme. [*E*] represents an external-facing free enzyme state. External Na^+ and K^+ binding take place at a locus within the membrane field. The ions must

Simplification of the Kinetic Equations by Adoption of the Hill Formalism

Of necessity, a major simplification has been made in the microscopic description of the ion binding process by the adoption of the Hill approximation. A more detailed microscopic model would account for the binding of each of the three Na^+ ions and two K^+ ions separately. It has been suggested, for example, that there are two negative charges on the enzyme to which Na^+ ions bind (De Weer, 1984; Nakao and Gadsby, 1986; Goldshlegger, Karlish, Rephaeli, and Stein, 1987). The first positively charged Na^+ that binds from the outside binds with high affinity and partially neutralizes the negative charges in the vicinity of the Na^+ ion binding sites, thereby reducing the affinity for binding of the second Na^+. The binding of the third Na^+ occurs with the lowest affinity. These interactions can be described in detail using a three-site model for Na^+ binding with negative cooperativity (Pedemonte, 1988). Since detailed information about the individual ion binding steps is not accessible by analysis of steady state *I-V* data, we have adopted the Hill formalism in which a multistate velocity equation with a high degree of cooperativity can be approximated by adoption of a noninteger value of the Hill coefficient (Segal, 1976). The Hill coefficients for Na^+ and K^+ are given the symbols γ_N and γ_K, respectively (see Appendix).

Reduction of the Three-State Model to a Pseudo Two-State Model

With the above definitions of the Hill coefficients and apparent well-depth for Na^+ and K^+, we may derive a steady state equation for the operation of the forward Na^+/K^+ pump cycle (Eq. A10) based on the three-state access channel model shown in Fig. 7 *A*. This equation can be reduced to an equivalent pseudo two-state equation (Eq. A14) by grouping the voltage- and concentration-independent rate constants of the three-state model as shown in Eqs. A15–A18. A similar simplification can be done for any multistate model in which only two oppositely directed rate coefficients are voltage dependent. In the pseudo two-state model shown in Fig. 7 *B* the backward voltage-dependent rate process is incorporated in the rate coefficient *b* (Eq. A12), the forward voltage-dependent rate process is incorporated in the rate coefficient *c* (Eq. A13), while *a* and *d* represent the result of combining the forward and backward voltage-independent rate constants of the multistate model, respectively. Since in the

---

pass through a fraction of the membrane field (λ_N and λ_K) before being bound. Equilibration of Na^+ and K^+ within the external access channel occurs rapidly as a Boltzmann distribution of voltage. The pseudo first-order rate coefficients k_{21} and k_{23} are voltage dependent as a result of the voltage dependence of the effective ion concentrations at their binding locus. Because the pump is primarily operating in the forward direction, k_{13} is assumed to be zero. The steady state current equation for this three-state model is given by Eq. A10. (*B*) Pseudo two-state model of steady-state operation of the Na^+/K^+ pump. Rate coefficients *b* and *c* are voltage dependent as a consequence of the location of Na^+ and K^+ binding sites within an external access channel. $[E]_i$ is the internal-facing enzyme state whereas $[E]_o$ is the external-facing enzyme. This model is sufficient to describe the *I-V* behavior of any irreversible unbranched cycle in which no more than two oppositely directed rate coefficients of the cycle are voltage dependent. Since the pump is primarily operating in the forward direction, *d* is assumed to be zero. The steady state current equation for this pseudo two-state model is given by Eq. A11.

experiments described here, we are considering only the steady state current generated by the forward-going Na^+/K^+ pump far from equilibrium, the backward rate constant d is assumed to be zero.

Steady State Current Equations for Various Experimental Cases

In Na^+-free solutions the pseudo two-state current equation (A14) can be reduced to Eq. A19 from which it is possible to obtain estimates for the parameters $FN\rho a$, $\bar{c}/a$, γ_K, and λ_K (Fig. 3). This is the simplest case to be considered from among the four cases to be discussed, and is sufficient to obtain a preliminary estimate of the value of λ_K. The dashed lines in Fig. 3 were obtained from a fit of Eq. A19 to the data from this case alone. A slight simplification of Eq. A14 can be made when $[K]_o$ is large (Eq. A26). Data from this case are shown in Fig. 4. Two additional cases considered that require the complete Eq. A14 are the activation of pump current by $[K]_o$ at 120 mM (Fig. 5) and 15 mM $[Na]_o$ (Fig. 6).

Overall Least-Squares Fit

A total of seven parameters or groups of parameters have been determined by a simultaneous nonlinear least squares fit of all of the *I-V* data to appropriate forms of the steady state current equation for each experimental case (Marquardt-Levenberg algorithm). Five parameters are common to all four experimental cases (Table I). The values of λ_N and λ_K may be thought of as the mean electrical distance at which Na^+ and K^+ bind, respectively. The Hill coefficient for Na^+ (γ_N) and the combinations of rate constants: $\bar{c}/a$ and $\bar{b}/\bar{c}$ are also common to all four cases. The two parameters that are not common to the different experimental cases are γ_K and I_{max}. γ_K varies systematically with $[Na]_o$ ranging from 0.581 ± 0.019 to 1.35 ± 0.034 for 0 and 120 mM Na^+, respectively (Table II). I_{max} was also different for each case to allow for variability in pump site density in different batches of oocytes (Table III).

Dielectric Coefficients

Because one net charge is transported outward across the membrane per pump cycle, the sum of the dielectric coefficients (Läuger and Apell, 1986; Läuger and Jauch, 1986; Läuger, 1991, p 66) for the pump cycle must be 1.0. Given the values of the parameters λ_N and λ_K obtained from the overall least-squares fit of 0.486 and 0.256, respectively, we can calculate dielectric coefficients for the movement of 3 Na^+ and 2 K^+ across these fractional dielectric distances. For the outward movement of 3 Na^+ across a mean well-depth of 0.486 ± 0.010 we obtain a dielectric coefficient for Na^+ translocation (α_N) of +1.458 ± 0.029. For the inward movement of 2 K^+ across a mean well-depth of 0.256 ± 0.009 we calculate a dielectric coefficient for K^+ translocation (α_K) of −0.512 ± 0.019. The sum $\alpha_N + \alpha_K = 0.946 \pm 0.048$ is in good agreement with the theoretical expectation of 1.0 for the net outward movement of one charge through the entire membrane field. That is, the apparent well-depths calculated from the kinetic data are consistent with the net charge translocation expected for a 3 Na^+/2 K^+ pump stoichiometry ($3\lambda_N - 2\lambda_K = 1$). This analysis, therefore, is consistent with the major charge translocating events during the Na^+/K^+ pump cycle being almost entirely due to the equilibration of Na^+ and K^+ within an

TABLE I

Pseudo Two-State Model Parameters Common to All Four Experimental Cases

Parameter	Value ± SE
λ_N	0.486 ± 0.010
λ_K	0.256 ± 0.009
γ_N	2.18 ± 0.06
$\bar{c}/a$	0.421 ± 0.023 $mM^{-\gamma_K}$
$\bar{b}/\bar{c}$	3.9 ± 1.2 × 10^{-5} $mM^{\gamma_K-\gamma_N}$

external access channel. The data, however, do not exclude the possible existence of other charge-translocating steps in the Na^+/K^+ pump cycle.

Mean Electrical Distances

The question arises of how to interpret the physical meaning of the parameters λ_N and λ_K. These parameters represent mean values of the individual fractional dielectric distances. Because the dielectric coefficients for Na^+ and K^+ movement are the sum of the individual dielectric coefficients we may write $3\lambda_N = \lambda_{N1} + \lambda_{N2} + \lambda_{N3}$ and $2\lambda_K = \lambda_{K1} + \lambda_{K2}$, where the doubly subscripted parameters represent the fractional dielectric distances for the individual ions. The steady state analysis gives us no information about how to separate the contribution of the individual ions. Thus we should interpret the value of $\lambda_K = 0.256$ determined from the overall fitting procedure to mean that each of the two transported K^+ ions bind at an average fractional dielectric distance of 0.256. Similarly, we may say that each Na^+ ion binds at an average fractional dielectric distance of 0.486. The steady state analysis does not tell us whether each of the three Na^+ ions bind at the same dielectric distance or whether, for example, one ion crosses almost the entire membrane field before binding while the other two cross only a small portion of the field. Evidence supporting this latter possibility has recently been obtained by Wuddel, Stürmer, and Apell (1993) by measurement of current transients induced by photochemical release of ATP from caged ATP. They find a dielectric coefficient associated with the release of the first Na^+ ion of 0.7, and dielectric coefficients for the subsequent release of the other two Na^+ ions of 0.2 for each ion.

TABLE II

$[Na]_o$ Dependence of the Hill Coefficient for K^+

$[Na]_o$	γ_K
mM	
120	1.35 ± 0.034
60	1.08 ± 0.024
30	0.911 ± 0.022
15	0.657 ± 0.022
7.5	0.62*
0	0.581 ± 0.019

*Interpolated value.

$[Na]_o$ Dependence of γ_K

It is well established that the Hill coefficient for activation of the Na^+/K^+ pump by $[K]_o$ increases as $[Na]_o$ is increased (Garrahan and Glynn, 1967; Baker, Blaustein, Keynes, Manil, Shaw, and Steinhardt, 1969; Rakowski et al., 1989). As $[Na]_o$ is decreased the apparent affinity for $[K]_o$ increases, causing a leftward shift of the K^+-activation curve and a decrease in the measured value of the Hill coefficient, γ_K. We, therefore, allowed γ_K to vary in experiments at different $[Na]_o$. The values of γ_K obtained by the overall least squares fitting procedure varied systematically in the manner expected from previous studies (Table II). Insufficient curvature in the data at 7.5 mM $[Na]_o$ in Fig. 4 required that the value of γ_K at this concentration be calculated by interpolation.

Calculation of Individual Rate Coefficients Given the Density of Pump Sites (N)

The grouped parameters *FNρa* represent the theoretical maximum pump current (I_{max}) that will result under conditions in which the voltage-dependent rate coefficients are no longer rate determining, but instead the pump cycle is rate limited by voltage-independent steps. Because there is considerable variability in the density of

TABLE III

Theoretical Value of I_{max} for Each Experimental Case That Was Not Normalized

FNρa	Experimental case
$\mu A\ cm^{-2}$	
1.46 ± 0.06	0 Na ΔK
1.96 ± 0.07	15 Na ΔK
0.992 ± 0.018	120 Na ΔK

pump sites in different oocytes (Schweigert, Lafaire, and Schwarz, 1988; Vasilets, Omay, Ohta, Noguchi, Kawamura, and Schwarz, 1991) *FNρa* was allowed to vary in the fit to each experimental case. No consistent trend in the value of FNρa is seen in Table III as $[Na]_o$ is increased. The variability in this group of parameters may arise from variability of the pump site density (N), or the reserve factor (ρ). The reserve factor is unity for simple models of pump operation such as the three-state model discussed in the Appendix. For more complex branched models, for example, ρ represents the amount of enzyme sequestered in voltage independent reactions (Hansen et al., 1981). The fact that *FNρa* is not constant for all experimental conditions, may be a result of recruitment of sequestered enzyme from a reserve pool. Rakowski (1993) has reported that the measured value of the total amount of pre–steady state charge moved under Na^+/Na^+ exchange conditions (Q_{tot}) increases as $[Na]_o$ is increased, suggesting that $[Na]_o$ is able to recruit more enzyme to participate in the slow electrogenic reactions from a nonparticipating pool.

Laying aside the potential complication introduced by the possible existence of an electrically silent reserve pool of enzyme, it is possible to estimate the value of the pseudo two-state rate constant (a) if we assume $\rho = 1$ and determine the pump site density. Vasilets et al. (1991) find values of pump site density of 330–360 μm^{-2} based on ouabain binding measurements. Using a value of 345 μm^{-2} and the mean value of *FNρa* from Table III of 1.5 $\mu A\ cm^{-2}$, a is calculated to be 270 s^{-1}.

The combinations of rate constants, $\bar{b}/\bar{c}$ and $\bar{c}/a$ should be independent of both $[Na]_o$ and $[K]_o$ and, therefore, a common value of each was used for all of the experimental conditions examined. From the least squares estimate of $\bar{c}/a$ of 0.421 ± 0.023 $mM^{-\gamma_K}$ and the above estimate of a, we can calculate $\bar{c}$ to be 110 $mM^{-\gamma_K}$ s^{-1}. From the least squares value of $\bar{b}/\bar{c}$ of 3.9 ± 1.2 × 10^{-5} $mM^{\gamma_K-\gamma_N}$ and the above estimate of $\bar{c}$, we calculate $\bar{b}$ to be 4.4 × 10^{-3} $mM^{-\gamma_N}$ s^{-1}.

The above analysis shows that it is possible to obtain the complete set of pseudo two-state model parameters from the nonlinear least squares fit of the steady state current equation to the data and a measurement of pump site density if the parameter ρ is assumed to be unity.

Comparison with Previous Results

Two of the parameters from the overall fit have an obvious physical meaning that allows comparison with results from other studies: λ_N and λ_K. The Hill coefficients (γ_N and γ_K) are kinetic parameters whose physical meaning is obscured by the assumption of the Hill formalism for multisite binding. The parameters, a, $\bar{b}$, and $\bar{c}$ correspond to collections of rate constants of higher-order models and are not directly comparable to individual rate constants available in the literature. A basis for comparison of values of λ_N and λ_K is provided by examination of values of the e-fold steepness factors and shifts of midpoint voltages for various voltage-dependent processes. For example, Gadsby et al. (1993) have recently reported a value of the fractional dielectric distance (λ) that describes the voltage dependence of unidirectional Na^+ efflux mediated by the Na^+/Na^+ exchange mode of operation of the Na^+/K^+ pump in squid giant axons. They find a value of λ of 0.69 ± 0.04 which is comparable to the value of λ_N of 0.486 ± 0.010 reported here. A comparison also can be made in the case of the fractional dielectric distance measured for K^+ binding. Rakowski et al. (1991) found an e-fold steepness for the apparent K_m for activation of pump current in Na^+-free solution of 0.37. The average Hill coefficient was 1.3 from which we may calculate a value of λ_K of 0.29. Bielen, Glitsch, and Verdonck (1993) found a value of 0.24 for the e-fold steepness and a Hill coefficient of 1.2. This gives an estimate of λ_K of 0.20. These values correspond well with the value of λ_K of 0.280 ± 0.007, obtained from the fit of Eq. A19 to the data in Fig. 3, and with the value of λ_K of 0.256 ± 0.009 obtained from the overall fit (Table I).

The rate constants measured by Nakao and Gadsby (1989) cannot be directly compared with the rate constants measured here. It is instructive, however, to calculate values of the rate coefficients b and c of the pseudo two-state model for particular values of $[Na]_o$, $[K]_o$, and V, and calculate the predicted pump turnover rate from Eq. A11 and the value of the voltage-independent theoretical maximum turnover rate a. From Eq. A12 we may calculate a value of b of 150 s^{-1} at 120 mM $[Na]_o$ and 0 mV, and from Eq. A13 we obtain a value of c of 285 s^{-1} at 2.5 mM $[K]_o$ and 0 mV. The pump turnover rate $ac/(a + b + c)$ can be calculated to be 110 s^{-1} under these conditions. This value is somewhat higher than might be expected from measurements of slow steps in the pump cycle in isolated mammalian enzyme. At 20°C the K^+ deocclusion rate to the inside is expected to be about 45 s^{-1} (Forbush, 1987) and the Na^+ deocclusion rate to the outside only ~20 s^{-1} (Stürmer, Apell, Wuddel, and Läuger, 1989).

Possible Sources of Experimental Error

The extensive sets of data analyzed here were collected using somewhat tedious and complicated protocols (Figs. 1 and 2) that, despite the difficulty of obtaining complete experiments of over 3 h in duration, have the advantage of allowing corrections to be made for run-down of the pump current magnitude and slight drifts in steady state current. These precautions should minimize drift and run-down as sources of experimental error. Two additional sources of error are the presence in the subtracted *I-V* data of non–pump-mediated K^+-sensitive current and of inward pump current. Appropriate control measurements are shown in Figs. 3 *C*, 5 *B*, and 6 *C* that demonstrate that non–pump-mediated K^+-sensitive current is no larger than $\sim 10\%$ of I_{max}. The DHO-sensitive current measured in the control experiments of Figs. 3 *B* and 6 *B* may, or may not, represent a more significant source of experimental error, particularly at hyperpolarized potentials. If this (mostly) inwardly directed current is present whether or not external K^+ is present, it will be eliminated by the subtraction procedure used to measure forward-going K^+-sensitive pump current. If, however, this current is K^+ sensitive, for example being largest in K^+-free solution and diminished by increasing $[K]_o$, the control measurements will give an estimate of the upper limit of the possible contamination of the records by this current. Since there is no way at present to decide between these two extremes and no means by which a correction can be applied to the data, we have simply chosen to ignore this possible source of experimental error until more is known about it.

Agreement of Theory and Data

The agreement between the theoretical curves and the data is quite good in Figs. 3–6, but there are systematic deviations of the data from the theory. This may be an indication that the theory does not sufficiently account for complexities that might arise, for example, if an additional step in the cycle were voltage dependent or if internal [Na] was not sufficiently maintained near saturation and thereby allowed a small voltage dependence at an internal-facing access channel to complicate the results. Karlish and Stein (1985) in experiments on pumps reconstituted in lipid vesicles and Nakao and Gadsby (1989) in myocytes have shown a small increase in the apparent affinity for internal Na^+ with depolarization, consistent with a shallow internal access channel for Na^+. Stürmer et al. (1991*a*, *b*) have also postulated the presence of such an internal access channel for Na^+ binding based on measurements with amphipathic fluorescent dyes.

The model developed in the Appendix does not account for several predictable effects of an external access channel. It assumes, for example, that the binding rate coefficients increase exponentially without limit. This, obviously, cannot be the case since saturation of channel occupancy will occur at sufficiently high substrate concentration or negative membrane potentials. Similarly, the model assumes complete asymmetry of the binding and release processes, with all of the voltage dependence falling on the binding rate coefficient. However, at high substrate concentration or sufficiently negative membrane potentials occupancy of the access channel will increase and electrostatically prevent dissociation of bound ions, leading to an apparent voltage dependence of the release rate.

The systematic deviations between the fit calculated from the model and the data suggest that the model could be improved by allowing the inclusion of additional

voltage-dependent steps within the pump cycle. Recent data obtained in squid giant axons (P. De Weer, D. C. Gadsby, and R. F. Rakowski, unpublished observations) suggest that there is a shallow voltage dependence of the steady state pump *I-V* relationship in Na^+-free solutions and at saturating $[K]_o$. Bielen et al. (1993) have also noted that there is a positive slope in the pump *I-V* relationship in cardiac Purkinje cells in Na-free solution at 5.4 mM external $[K^+]$. Such a result cannot be explained based solely on external access channels since external Na is absent and external K^+ is saturating. We, therefore, recognize that the simple access channel model discussed here may require modification as more data become available. However, because the major features of the steady-state *I-V* data are reasonably well described, the access channel model provides a foundation for further studies and a convenient means of comparing data sets obtained with different functional mutations of the pump molecule that can be expressed in *Xenopus* oocytes.

APPENDIX

Relationship between the Fractional Field Distance (λ) for an Access Channel and the Rate Coefficients for Ion Binding

We may write the following Boltzmann expressions for the effective concentration of Na^+ and K^+ at their external binding locus (λ):

$$[Na]_\lambda = [Na]_o \exp(-\lambda_N U) \tag{A1}$$

$$[K]_\lambda = [K]_o \exp(-\lambda_K U) \tag{A2}$$

where $[Na]_o$ and $[K]_o$ are the external bulk solution concentrations of Na^+ and K^+, λ_N and λ_K represent the fraction of the membrane potential sensed by external Na^+ and K^+ at their binding locus, respectively, and $U = FV/RT$, where V is the membrane potential and F, R, and T have their usual meanings. Assuming rapid equilibration of Na^+ and K^+ within an external access channel we may write the following expressions for the pseudo first-order rate coefficients for binding of γ_N Na^+ and γ_K K^+ ions to external-facing free enzyme ($[E]$) for the reaction scheme shown in Fig. 7 *A*:

$$k_{21} = \bar{k}_{21}[Na]_o^{\gamma_N} \exp(-\lambda_N \gamma_N U) \tag{A3}$$

$$k_{23} = \bar{k}_{23}[K]_o^{\gamma_K} \exp(-\lambda_K \gamma_K U) \tag{A4}$$

where $\bar{k}_{21}$ and $\bar{k}_{23}$ represent the rate constants at $V = 0$, and γ_N and γ_K are the Hill coefficients for Na^+ and K^+, respectively.

I-V *Relationship for a Three-State External Access Channel Model*

The following differential equations may be written for the transitions between enzyme states for the reaction scheme shown in Fig. 7 *A* assuming that k_{13} is zero:

$$\frac{d[ENa]}{dt} = k_{31}[EK] + \bar{k}_{21}[Na]_o^{\gamma_N}[E] \exp(-\gamma_N \lambda_N U) - k_{12}[ENa] \tag{A5}$$

$$\frac{d[EK]}{dt} = \bar{k}_{23}[K]_o^{\gamma_K}[E] \exp(-\gamma_K \lambda_K U) - k_{32}[EK] - k_{31}[EK] \tag{A6}$$

$$\frac{d[E]}{dt} = k_{12}[ENa] + k_{32}[EK] - \bar{k}_{21}[Na]_o^{\gamma_N}[E] \exp(-\gamma_N \lambda_N U) - \bar{k}_{23}[K]_o^{\gamma_K}[E] \exp(-\gamma_K \lambda_K U) \tag{A7}$$

We define N to be the total amount of enzyme expressed in units of moles per square centimeter of membrane area:

$$N = [E\mathrm{Na}] + [E\mathrm{K}] + [E]. \tag{A8}$$

The steady state current (I) generated by forward operation of the reaction cycle is given by

$$I = k_{31} FN(E\mathrm{K}]. \tag{A9}$$

Because in the steady-state, $d[E\mathrm{Na}]/dt = \mathrm{d}[E\mathrm{K}]/\mathrm{d}t = \mathrm{d}[E]/\mathrm{d}t = 0$, Eqs. A5–A9 may be combined to give

$$I = \frac{FN}{\frac{1}{k_{31}} + \frac{1}{k_{12}} + \frac{(k_{32} + k_{31})}{k_{31}\bar{k}_{23}[\mathrm{K}]_o^{\gamma_K} \exp(-\gamma_K \lambda_K U)} + \frac{(k_{32} + k_{31})\bar{k}_{21}[\mathrm{Na}]_o^{\gamma_N} \exp(-\gamma_N \lambda_N U)}{k_{31}k_{12}\bar{k}_{23}[\mathrm{K}]_o^{\gamma_K} \exp(-\gamma_K \lambda_K U)}} \tag{A10}$$

Steady State I-V *Relationship for a Pseudo Two-State Access Channel Model*

The pseudo two-state reaction scheme shown in Fig. 7 *B* gives the following general solution for pump current (Hansen et al., 1981; Läuger, 1991, p. 73):

$$I = FN\rho \frac{ac - bd}{a + b + c + d} \tag{A11}$$

For an irreversible forward-going pump cycle we may assume that $d = 0$. Given an external access channel for Na^+ and K^+ binding we may write

$$b = \bar{b}[\mathrm{Na}]_o^{\gamma_N} \exp(-\gamma_N \lambda_N U) \tag{A12}$$

$$c = \bar{c}[\mathrm{K}]_o^{\gamma_K} \exp(-\gamma_K \lambda_K U) \tag{A13}$$

where $\bar{b}$ and $\bar{c}$ are the rate constants at $V = 0$. Substitution of Eqs. A12 and A13 into A11 and setting $d = 0$ gives

$$I = \frac{FN\rho a}{1 + \frac{a + \bar{b}[\mathrm{Na}]_o^{\gamma_N} \exp(-\gamma_N \lambda_N U)}{\bar{c}[\mathrm{K}]_o^{\gamma_K} \exp(-\gamma_K \lambda_K U)}} \tag{A14}$$

Equivalence of the Pseudo Two-State and Three-State Access Channel Models

Inspection of Eqs. A10 and A14 shows that the pseudo two-state and three-state models are equivalent if the following parameter assignments are made

$$\rho = 1 \tag{A15}$$

$$a = \frac{k_{31}k_{12}}{k_{31} + k_{12}} \tag{A16}$$

$$\bar{b} = \frac{k_{31}\bar{k}_{21}}{k_{31} + k_{12}} \tag{A17}$$

$$\bar{c} = \frac{k_{31}\bar{k}_{23}}{k_{32} + k_{31}} \tag{A18}$$

It can also be demonstrated that the addition of enzyme states in Fig. 7*A* with voltage-independent rate constants leads to current equations that can be reduced to Eq. A11 if appropriate assignment of parameters are made. We conclude, therefore, that equations having the general form of Eq. A11 are sufficient to describe the *I-V* behavior of any irreversible unbranched cycle in which two oppositely directed rate coefficients of the cycle are voltage dependent. This special case in which only two oppositely directed rate coefficients are voltage dependent, therefore, is equivalent to a class I model defined by Hansen et al. (1981) despite the fact that there are two distinct voltage dependent steps.

Simplification of the I-V *Relationship when* $[Na]_o = 0$

An experimentally useful simplification of the *I-V* relationship can be achieved when $[Na]_o = 0$. In this case Eq. A14 becomes

$$I = \frac{FN\rho a}{1 + \dfrac{a}{\bar{c}[K]_o^{\gamma_K} \exp(-\gamma_K \lambda_K U)}} \tag{A19}$$

Eq. A19 can be simplified if we define a theoretical maximum current $I_{max} = FN\rho a$ so that I/I_{max} is

$$\frac{I}{I_{max}} = \frac{1}{1 + \dfrac{a}{\bar{c}[K]_o^{\gamma_K} \exp(-\gamma_K \lambda_K U)}} \tag{A20}$$

Eq. A20 can be reduced to a Boltzmann equation by defining $\overline{U}_K$

$$\exp(-\gamma_K \lambda_K \overline{U}_K) = \frac{a}{\bar{c}[K]_o^{\gamma_K}} \tag{A21}$$

Substituting the left-hand side of Eq. A21 in Eq. A20 gives

$$\frac{I}{I_{max}} = \frac{1}{1 + \exp[\gamma_K \lambda_K (U - \overline{U}_K)]} \tag{A22}$$

which is a Boltzmann equation that saturates at extreme negative potentials and whose exponential steepness is related to $\gamma_K \lambda_K$.

An alternative simplification to a Hill form of equation can be obtained by defining

$$K_K^{\gamma_K} = \left(\frac{a}{\bar{c}}\right) \exp(\gamma_K \lambda_K U) \tag{A23}$$

Substitution of Eq. A23 into A20 gives a Hill equation of the following form:

$$\frac{I}{I_{max}} = \frac{[K]_o^{\gamma_K}}{[K]_o^{\gamma_K} + K_K^{\gamma_K}} \tag{A24}$$

Simplification of the I-V *Relationship when* $[Na]_o$ *Is Fixed*

Eq. A14 does not simplify to a Boltzmann equation when both external Na^+ and K^+ are present at low concentrations. Eq. A14, however, has the form of the Hill equation where $FN\rho a$ is the theoretical maximum current determined by voltage independent rate processes, and the

half-saturation concentration (K_K) is defined as follows:

$$K_K^{\gamma_K} = \frac{a + \bar{b}[Na]_o^{\gamma_N} \exp(-\gamma_N \lambda_N U)}{\bar{c} \exp(-\gamma_K \lambda_K U)} \tag{A25}$$

Substitution of $I_{max} = FN\rho a$ and A25 into Eq. A14 gives the Hill equation (A24). Note, however, that in this case the voltage dependence of K_K is complex.

I-V *Relationships for Large Values of* $[K]_o$

For large values of $[K]_o$ the term $a/(\bar{c}\,[K]_o^{\gamma_K} \exp[-\gamma_K \lambda_K U])$ in Eq. A14 becomes small compared to 1 so that the equation may be simplified to give:

$$I = \frac{FN\rho a}{1 + \dfrac{\bar{b}[Na]_o^{\gamma_N} \exp(-\gamma_N \lambda_N U)}{\bar{c}[K]_o^{\gamma_K} \exp(-\gamma_K \lambda_K U)}} \tag{A26}$$

Eq. A26 is an inhibitory form of the Hill equation, if we let $I_{max} = FN\rho a$ and define a half-inhibitory concentration for Na^+ (K_N) as follows:

$$K_N^{\gamma_N} = \frac{\bar{c}[K]_o^{\gamma_K} \exp(-\gamma_K \lambda_K U)}{\bar{b} \exp(-\gamma_N \lambda_N U)} \tag{A27}$$

Substitution of these expressions in Eq. A26 gives

$$\frac{I}{I_{max}} = \frac{K_N^{\gamma_N}}{K_N^{\gamma_N} + [Na]_o^{\gamma_N}} \tag{A28}$$

Eq. A26 may also be written as a Boltzmann relationship.

We thank Drs. Paul De Weer, David C. Gadsby, and Hans-Jürgen Apell for helpful discussion and advice, Dr. Clifford Slayman for comments on the Appendix, Vivian Wallner for technical assistance, and Kim Cooprider for secretarial assistance.

Supported by NIH grant NS-22979.

Original version received 19 April 1993 and accepted version received 18 November 1993.

REFERENCES

Andersen, O. S., J. E. N. Silveira, and P. R. Steinmetz. 1985. Intrinsic Characteristics of the proton pump in the luminal membrane of a tight urinary epithelium. *Journal of General Physiology.* 86:215–234.

Baker, P. F., M. P. Blaustein, R. D. Keynes, J. Manil, T. I. Shaw, and R. A. Steinhardt. 1969. The ouabain-sensitive fluxes of sodium and potassium in squid giant axons. *Journal of Physiology.* 200:459–496.

Bielen, F. V., H. G. Glitsch, and F. Verdonck. 1993. Na^+ pump current-voltage relationships of rabbit cardiac Purkinje cells in Na^+-free solution. *Journal of Physiology.* 465:699–714.

De Weer, P. 1984. Electrogenic pumps: theoretical and practical considerations. *In* Electrogenic Transport: Fundamental Principles and Physiological Implications. M. P. Blaustein and M. Lieberman, editors. *Society of General Physiologists Series.* 38:1–15.

Eisner, P. A., M. Valdeolmillos, and S. Wray. 1987. The effects of membrane potential on active and passive Na transport in *Xenopus* oocytes. *Journal of Physiology.* 385:643–659.

Forbush, B. III. 1987. Rapid release of ^{42}K or ^{86}Rb from an occluded state of the Na, K-pump in the presence of ATP or ADP. *Journal of Biological Chemistry.* 262:11104–11115.

Gadsby, D. C., M. Nakao, A. Bahinski, G. Nagel, and M. Suenson. 1992. Charge movements via the cardiac Na, K-ATPase. *Acta Physiologica Scandinavica.* 146:111–123.

Gadsby, D. C., R. F. Rakowski, and P. De Weer. 1993. Extracellular access to the Na,K pump: pathway similar to ion channel. *Science.* 260:100–103.

Garrahan, P. J., and I. M. Glynn. 1967. Factors affecting the relative magnitudes of the sodium: potassium and sodium:sodium exchanges catalyzed by the sodium pump. *Journal of Physiology.* 192:189–216.

Goldshlegger, R., S. J. D. Karlish, A. Rephaeli, and W. D. Stein. 1987. The effect of membrane potential on the mammalian sodium-potassium pump reconstituted into phospholipid vesicles. *Journal of Physiology.* 387:331–355.

Hansen, U.-P., D. Gradmann, D. Sanders, and C. L. Slayman. 1981. Interpretation of current-voltage relationships for "active" ion transport systems. I. Steady-state reaction-kinetic analysis of class-I mechanisms. *Journal of Membrane Biology.* 63:165–190.

Karlish, S. J. D., and W. Stein. 1985. Cation activation of the pig kidney sodium pump: transmembrane allosteric effects of sodium. *Journal of Physiology.* 359:119–149.

Lafaire, A. V., and W. Schwarz. 1986. Voltage dependence of the rheogenic Na^+/K^+ ATPase in the membrane of oocytes of *Xenopus laevis*. *Journal of Membrane Biology.* 91:43–51.

LaTona, J. 1990. Ion concentration and voltage dependence of Na/K pump current in *Xenopus laevis* oocytes. Ph.D. thesis. The University of Health Sciences/The Chicago Medical School, North Chicago, IL. University Microfilms, Ann Arbor, MI. 1–84.

Läuger, P. 1991. Electrogenic Ion Pumps. Sinauer Associates, Inc., Sunderland, MA. 313 pp.

Läuger, P., and H.-J. Apell. 1986. A microscopic model for the current-voltage behavior of the Na, K pump. *European Biophysics Journal.* 13:309–321.

Läuger, P., and P. Jauch. 1986. Microscopic description of voltage effects on ion-driven cotransport systems. *Journal of Membrane Biology.* 91:275–284.

Nakao, M., and D. C. Gadsby. 1986. Voltage dependence of Na translocation by the Na/K pump. *Nature.* 323:628–630.

Nakao, M., and D. C. Gadsby. 1989. [Na] and [K] dependence of the Na/K pump current-voltage relationship in guinea pig ventricular myocytes. *Journal of General Physiology.* 94:539–565.

Pedemonte, C. H. 1988. Kinetic mechanism of inhibition of the Na^+-pump and some of its partial reactions by external Na^+ (Na_o^+). *Journal of Theoretical Biology.* 134:165–182.

Rakowski, R. F. 1993. Charge movement by the Na/K pump in *Xenopus* oocytes. *Journal of General Physiology.* 101:117–144.

Rakowski, R. F., D. C. Gadsby, and P. De Weer. 1989. Stoichiometry and voltage dependence of the sodium pump in voltage-clamped, internally dialyzed squid giant axon. *Journal of General Physiology.* 93:903–941.

Rakowski, R. F., and C. L. Paxson. 1988. Voltage dependence of Na/K pump current in *Xenopus* oocytes. *Journal of Membrane Biology.* 106:173–182.

Rakowski, R. F., L. A. Vasilets, J. LaTona, and W. Schwarz. 1991. A negative slope in the current-voltage relationship of the Na^+/K^+ pump in *Xenopus* oocytes produced by reduction of external $[K^+]$. *Journal of Membrane Biology.* 121:177–187.

Sagar, A., and R. F. Rakowski. 1993. Access channel model for the activation by external [K] of the Na/K pump in *Xenopus* oocytes. *FASEB Journal.* 7:A580. (Abstr.)

Sagar, A., V. Wallner, and R. F. Rakowski. 1993. Current-voltage relationships of the Na/K pump in *Xenopus* oocytes analyzed using an access channel model. *Biophysical Journal.* 64:A332. (Abstract)

Schweigert, B., A. V. Lafaire, and W. Schwarz. 1988. Voltage dependence of the Na-K ATPase: measurements of ouabain-dependent membrane current and ouabain binding in oocytes of *Xenopus laevis*. *Pflügers Archiv.* 412:579–588.

Segal, I. H. 1976. Biochemical Calculations. Second edition. John Wiley & Sons, Inc., New York. 309.

Stürmer, W., H.-J. Apell, I. Wuddel, and P. Läuger. 1989. Conformational transitions and charge translocation by the Na, K-pump: comparison of optical and electrical transients elicited by ATP-concentration jumps. *Journal of Membrane Biology.* 110:67–86.

Stürmer, W., R. Bühler, H.-J. Apell, and P. Läuger. 1991*a*. Charge translocation by the Na,K-pump. II. Ion binding and release at extracellular face. *Journal of Membrane Biology.* 121(2):163–76.

Stürmer, W., R. Bühler, H.-J. Apell, and P. Läuger. 1991*b*. Charge translocation by the sodium pump: ion binding and release studied by time-resolved fluorescence measurements. *In* The Sodium Pump: Recent Developments. J. H. Kaplan and P. De Weer, editors. Rockefeller University Press, New York. 531–536.

Vasilets, L. A., T. Ohta, S. Naguchi, M. Kawamura, and W. Schwarz. 1993. Voltage-dependent inhibition of the sodium pump by external sodium: species differences and possible role of the N-terminus of the α-subunit. *European Biophysics Journal.* 21:433–443.

Vasilets, L. A., H. S. Omay, T. Ohta, S. Noguchi, M. Kawamura, and W. Schwarz. 1991. Stimulation of the Na^+/K^+ pump by external $[K^+]$ is regulated by voltage-dependent gating. *Journal of Biological Chemistry.* 266:16285–16288.

Wu, M. W., and M. M. Civan. 1991. Voltage dependence of current through the Na,K-exchange pump of *Rana* oocytes. *Journal of Membrane Biology.* 121:23–36.

Wuddel, I., W. Stürmer, and H.-J. Apell. 1993. Dielectric coefficients of the extracellular release of sodium ions. *Biological Chemistry Hoppe-Seyler.* 374:596 (Abstract).